

Original article

Optimization of a pharmacophore model for 5-HT₄ agonists using CoMFA and receptor based alignmentMagdy N. Iskander^{a,*}, Lok M. Leung^a, Trevor Buley^a, Fadi Ayad^a, Juliana Di Iulio^b,
Yean Y. Tan^b, Ian M. Coupar^b^a The Department of Medicinal Chemistry, Victorian College of Pharmacy, Monash University, 381 Royal Parade, Parkville, Vic. 3052, Australia^b The Department of Pharmaceutical Biology and Pharmacology, Victorian College of Pharmacy,
Monash University, 381 Royal Parade, Parkville, Vic. 3052, Australia

Received 5 April 2005; accepted 13 July 2005

Available online 15 November 2005

Abstract

Twenty two 5-HT₄ agonists obtained from our laboratory and the recent literature were used to develop a CoMFA model to predict 5-HT₄ agonist activity. Two models were produced and compared for predictivity, the first by alignments based on atom overlapping (model A) and the second by adding agonist binding site interacting points of the 5-HT₄ receptor (model B). Comparison of the two models showed that the q^2 value for model A was 0.564 vs. 0.582 for model B. Model B indicated that the predictive power model stems from far lower steric contributions, 0.270 compared to model A's 0.502. The dominant defining features were the electrostatic contributions for model B, 0.664 up from 0.477 in model A. The contributions from the LogP factor were minimal, 0.085 in both models. The synthesized compounds showed agonist activity at μ mol level.

© 2005 Elsevier SAS. All rights reserved.

Keywords: 5-HT₄; Agonist; Receptor; CoMFA; 5-Hydroxytryptamine

1. Introduction

5-Hydroxytryptamine (5-HT) is involved in controlling an array of physiological functions and in promoting pathophysiological conditions in states of excess or deficiency. Fourteen receptors for 5-HT have been cloned. All, with the exception of 5-HT₃ (an ion channel) and 5-HT_{5B} (unknown coupling), are members of the GPCR superfamily of membrane-bound receptors [1]. A major relevance of the 5-HT₄ receptor is its involvement in controlling several functions of the human large intestine. A population of 5-HT₄ receptors is localized in the circular smooth muscle layer where their stimulation by endogenous 5-HT or 5-HT₄ agonists leads to relaxation [2] utilizing the adenylyl cyclase signal transduction system [3]. 5-HT₄ receptors are also located in the mucosa of the colon where their function is to promote Cl⁻ secretion with associated fluid loss from the lumen [4]. They are also present on cholinergic nerve

endings to facilitate colonic propulsion [5] and on sensory nerve endings where their function is thought to enhance sensory perceptions arising from the abdomen. Therefore, the 5-HT₄ receptor has been identified as a therapeutic target for treating irritable bowel syndrome (IBS) using selective agonists with limited success to date [6,7]. The functional characterization of 5-HT₄ receptors is based on both agonist and antagonist activities and has been extensively reviewed [8]. 5-HT₄ receptor agonists include indoleamine derivatives such as 5-methoxytryptamine (5-MeOT) and 5-carboxyamidotryptamine (5-CT); the substituted benzamide derivatives such as cisapride, renzapride and zacopride; the benzimidazolone derivatives BIMU 1, BIMU 8 and DAU 6236 and the substituted pyrrolizidine SC 53116. Only a small number of 5-HT₄ agonists are used clinically. Examples are the relatively non-selective agonists cisapride and metoclopramide and the recently introduced selective partial agonist tegaserod for treating constipation predominant IBS in female patients. These drugs have relatively low potency when compared to the natural ligand. Therefore, it is important to develop more potent and selective

* Corresponding author. Tel.: +61 3 9903 9679; fax: +61 3 9903 9545.
E-mail address: magdy.iskander@vcp.monash.edu.au (M.N. Iskander).

agents with better pharmacological and side effect profiles than those currently available.

Previous studies in our laboratories have resulted in a pharmacophore model based on the molecular structural and pharmacological properties of known agonists [9]. The pharmacophore model was developed using seven known active agonists, indolecarbazimidamide, 3-*N*-isopropylbenzimidazolone amide, 3-*N*-ethylbenzimidazolone amide and benzamide, *R*-zacopride, 5-CT and metoclopramide. Extensive study of the X-ray structures of these agonists and closely-related compounds, identified important interactions constraining the conformational flexibility of the side chains of the agonists. This knowledge, together with molecular mechanics optimization methods, allowed us to deduce the likely binding conformations of the agonists at the 5-HT₄ agonist binding site. Superimposition of the agonists was carried out using atom-by-atom fit with respect to 5-HT. This alignment was used to develop CoMFA models of the likely 5-HT₄ agonist binding site. The models were predictive with cross-validated q^2 values of 0.26–0.51 and final r^2 values of 0.96–0.99. Steric, electrostatic and lipophilic properties of the agonist were all found to be important. The final model identified regions in 3D property space which were important for modulating the activity of agonists. Consequently, several agonist compounds were designed and their structures were based on the developed pharmacophore recommendations. The pharmacological evaluation of these agonists was carried out using the guinea pig ileum, which is a standard bioassay for 5-HT₄ ligands. The present CoMFA study included these compounds together with 5-HT and the 5-HT₄-preferring agonists (**1–6**, **10–15**, **17** and **18**, Table 1) to achieve more defined agonist site characteristics.

2. Experimental methods

CoMFA [15,16] has been used to develop predictive models to describe the 3D structure–activity relationship for the compounds of interest based on their steric and electrostatic variations. The training and test sets used to generate the CoMFA models consisted of 5-HT, literature compounds (**1–6**, **10–15** and **17** and **18**) and our compounds (**7–9**, **16**, and **19–22**), Table 1. The design of our synthesized compounds was based on our early model [9]. Their biological evaluations were also carried out in our laboratory.

3. CoMFA model generation

All computation tasks were carried out using the SYBYL 6.9 molecular modeling package [17] running on a SGI R5000 workstation. Structures were minimized using the MMFF94s Force Field and MMFF94 [18,19] charges to a convergence criterion of 0.01 kcal/mol. All valencies were filled with hydrogens or lone pairs.

Pharmacophore sites were identified and aligned using the oxygen atom of the 5-hydroxyl group, the centroid of the aromatic ring and the nitrogen atom of the indolyl group as the

template (Fig. 1c). Relative potencies and log *P* values were assembled from literature values and from our experimental results. The steric and electrostatic CoMFA fields were generated separately, with truncated energy at 30 kcal/mol and scaled to equalize their weighting in the CoMFA models; standard CoMFA scaling. A region was created with boundaries extending 4 Å beyond the largest structure in all directions using a sp³ probe carrying a unit positive charge. One Å grid spacing was used with 1728 lattice points to compare the molecular details.

PLS, leave-one-out (LOO) method regression analysis [20] was used in conjunction with cross-validation to obtain the optimal number of components to be used in the subsequent analyses. A subset of CoMFA field sample points falling within a standard deviation of ≤ 2.0 kcal/mol was used to perform PLS regression analysis. The optimum number of principle components in the final non-cross-validated QSAR equations was determined to be that leading to the highest correlation (q^2) and the lowest standard error (Scv) in the LOO cross and validated predictions. The non-cross-validation was used in the analysis of the CoMFA results and the predictions.

4. Results and discussion

CoMFA is a 3D-QSAR method that operates on a set of ligands that have been superimposed to reflect their anticipated common binding orientation. A bioactive conformation must be energetically favorable and common among all active compounds having the same binding mode. In this investigation two CoMFA analyses were developed and compared in order to achieve a predictive model to improve our earlier pharmacophore [9] for agonist activity. The methods of fitting for the two separate models vary with a few key points.

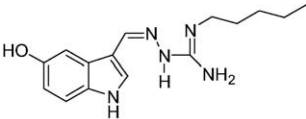
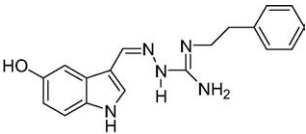
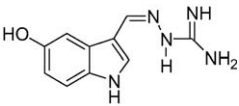
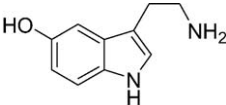
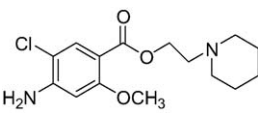
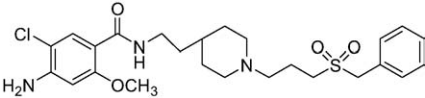
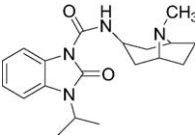
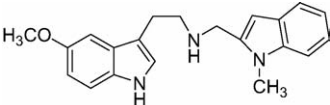
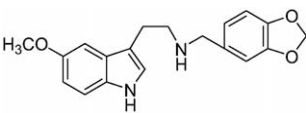
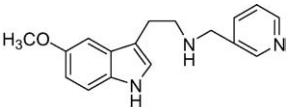
4.1. CoMFA model A (alignment based on atom overlapping)

In this CoMFA model a structural superimposition template was used with the positions of the 5-hydroxyl oxygen, the centroid of the adjacent aromatic ring and the charged indolyl amine ~ 8 Å from the hydroxyl as the key points for fitting. The molecules were superimposed using the SYBYL fit atom routine, using the key molecular points listed above.

This template worked well for all compounds with the 5-HT scaffold, however it was difficult to properly fit agonists with different scaffold e.g. BIMU 8, ML 10302 and 2-[(4-acetamidopiperidinyl)ethyl]-4-amino-5-chloro-2-methylbenzoate. These agonists do not have a hydroxyl group adjacent to the aromatic ring and the distant nitrogens (atom equivalent to the side chain indolyl N) and they vary significantly in their coordinates relative to the central aromatic ring. However, molecules that did not contain one or more of the key atoms were superimposed using the remaining key atoms and alternate features of similar conformation to the 5-HT template. Additionally, compounds **1** and **2** were torsionally adjusted away from their global minima conformation to one of the local minima in order to fit the 5-HT template optimally (Fig. 1).

Table 1

Structures of 5-HT₄ agonists used in the current studies. They consist of literature compounds (**1–6**, **10–15**, **17**, **18**, **21** and 5-HT) and compounds designed and synthesized in our laboratory (**7–8**, **16**, **19**, **20** and **22**).

Compound	Structure	Relative potency	E_{\max}	log P
#N-pentyl-3-[(5-hydroxy-1H-indol-3-yl)methylene] carbazimadamide (1) [10]		7.96	0.90	2.47
N-phenylethyl-3-[(5-hydroxy-1H-indol-3-yl)methylene] carbazimadamide (2) [10]		5.01	1.00	2.89
3-[(5-Hydroxy-1H-indol-3-yl)methylene] carbazimadamide (3) [10]		2.51	1.50	0.62
5-HT		1.00	1.00	0.05
ML 10302 (4) [11]		1.00	0.80	1.96
YM-36912 (5) [12]		0.91	0.90	3.23
BIMU 8 (6) [13]		0.71	1.00	3.65
(7)		0.69	0.72	3.35
(8)		0.65	0.59	3.38
(9)		0.62	0.91	3.42

(continued)

Table 1 (continued)

Compound	Structure	Relative potency	E_{\max}	$\log P$
2-[(4-Acetamido piperidinyl) ethyl]-4-amino-5-chloro-2-methoxybenzoate (10) [11]		0.38	0.59	0.60
5-MeOT (11)		0.25	1.00	0.53
DAU 6236 (12) [13]		0.21	1.00	3.55
Zacopride (13) [14]		0.01	0.80	1.23
5-CT (14) [14]		0.01	1.00	-0.21
Cisapride (15) [14]		0.008	0.70	2.58
(16)		0.005	0.50	1.03
Metoclopramide (17) [10]		0.002	1.00	1.61
YM-47813 (18) [12]		0.001	1.00	2.29
(19)		0.0005	0.42	0.85

(continued)

Table 1 (continued)

Compound	Structure	Relative potency	E_{\max}	$\log P$
(20)		0.0003	1.00	2.69
5-Benzyloxytryptamine (21)		0.0003	1.00	2.69
(22)		0.0003	0.60	1.08

#N-pentyl-3-[(5-hydroxy-1H-indol-3-yl)methylene] carbazimidamide (**1**) has been chosen for this study because of its known activity in the guinea pig myenteric plexus, however the actual drug compound is N-pentyl-3-[(5-methoxy-1H-indol-3-yl)methylene] carbazimidamide.

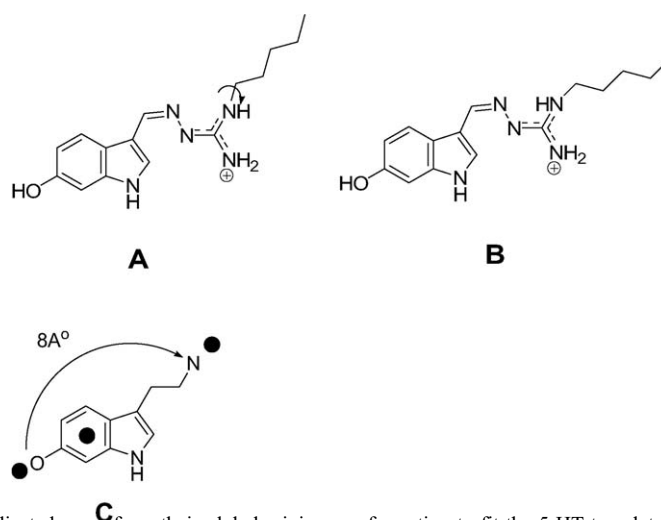


Fig. 1. Ligands **1** and **2** are torsionally adjusted away from their global minima conformation to fit the 5-HT template optimally. (a) Compound **1** is showing the global minima planar with the guanidine group, $\Delta E = -9.48$. (b) After 60° anticlockwise rotation of the N-C, $\Delta E = -9.17$. and (c) The template used for CoMFA analysis.

Thus, when an alignment was performed, groups beyond the atoms used to define the alignment spread greatly in model A. The pharmacophore features closest to the points of fitting are a clearly defined region beyond the 5-hydroxyl where steric bulk is unfavorable, an area above the 5-hydroxyl favoring positive electrostatic charge and a negative charge around the distant nitrogen (Fig. 2).

However, the less adequate fitting can be seen clearly in Fig. 3, where three agonists, two of which fit well based on the 5-HT scaffold (compounds **1** and **7**) and one which does not (compound **4**). A wide spread of side chains shows up in the features of the pharmacophore model; beyond the distant nitrogen however, the wide spread fit of the side chains is expressed in the pharmacophore model as an virtually random grouping of CoMFA regions, favored and unfavored steric

bulk overlapping along with a scattering of favored and unfavored electrostatic regions.

Such a diversity of fields affects the predictive power of the pharmacophore model A for the region beyond the distant nitrogen where all the variable side chains exist. Thus it was necessary to create a new agonist alignment and pharmacophore model to accommodate a variety of structures and improve the predictive ability of the model. The obtained data for model A are in Table 2 column A.

4.2. CoMFA model B (alignment based on receptor binding site)

The second CoMFA model (B) was developed by combining the first alignment of model A and the alignment based on

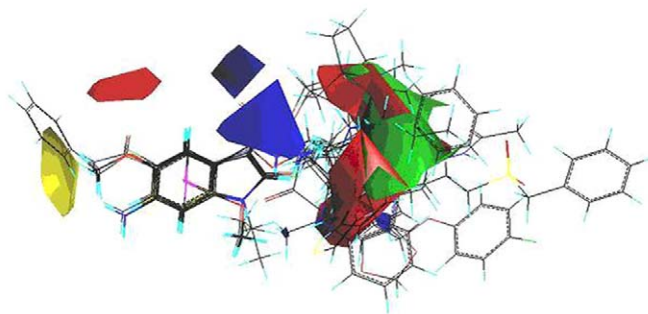


Fig. 2. The pharmacophore features developed from CoMFA model A using the complete dataset; all the 23 compounds from Table 1: blue regions favor negative electrostatic charge, red regions favor positive electrostatic charge, yellow regions where steric bulk is unfavorable and regions of favored steric bulk are colored green.

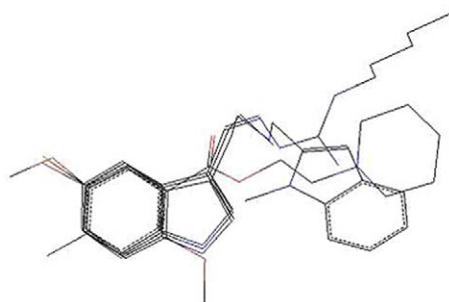


Fig. 3. CoMFA model A pharmacophore. Reduced dataset shown for simplicity, compounds shown are **1**, **4**, **7** and 5-HT.

Table 2
CoMFA analysis data of our early work [9], model A and model B

Model	Data from Ref. [9]	A	B
LOO cross validated q^2 value	0.570	0.564	0.582
Correlation coefficient r^2	0.994	0.974	0.994
Principal components n	3	6	8
<i>Contributions</i>			
Steric	0.352	0.502	0.270
Electrostatic	0.419	0.477	0.664
Lipophilic (log P)	0.228	0.052	0.085

the model of the agonist site of the 5-HT₄ receptor [21]. This approach was adopted to accommodate a variety of agonist structures in one pharmacophore. The molecular model of the 5-HT₄ agonist site was created from the crystal structure of bovine rhodopsin [22,23]. The 5-HT₄ receptor model indicated that hydrophobic interactions of the central aromatic ring were of less significance when compared to the electrostatic interactions between the 5-hydroxyl and serine 197 and the charged indolyl amine and aspartic acid 100 (Fig. 4).

Test compounds that did not share a common structure were superimposed via the strongest match of electrostatic points, such as the carboxyl oxygen and secondary amine in the compounds zacopride, cisapride and metoclopramide (Fig. 5). While some regions of the alignment model B may appear more complex, they play no direct part in predictive agonist activity. The regions in model B are clearly defined areas of favorable negative charge (Fig. 5) and an extremely well defined narrow region of favorable steric bulk (Fig. 6).

The region to the left and below of the 5-hydroxy anchor point were shown to have no predictive power in model B pharmacophore (Figs. 5 and 6). In Figs. 5 and 6 all fields are much better refined with better alignment, larger in most cases, better shape definition (circular or spherical) and the region

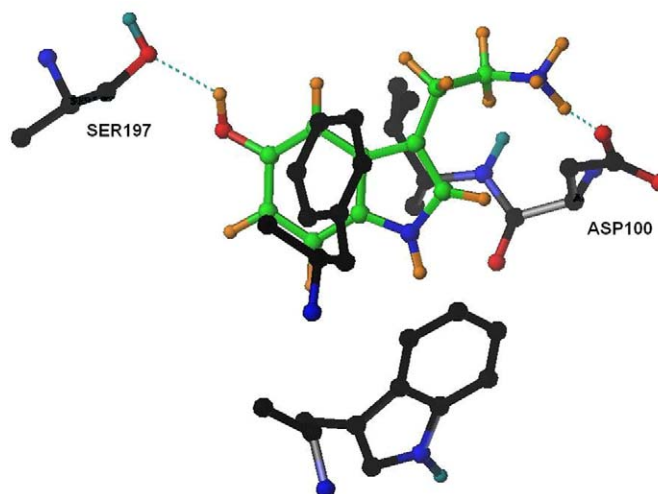


Fig. 4. 5-HT (green) bound in the receptor site with the two anchoring points; SER 197 and ASP 100.

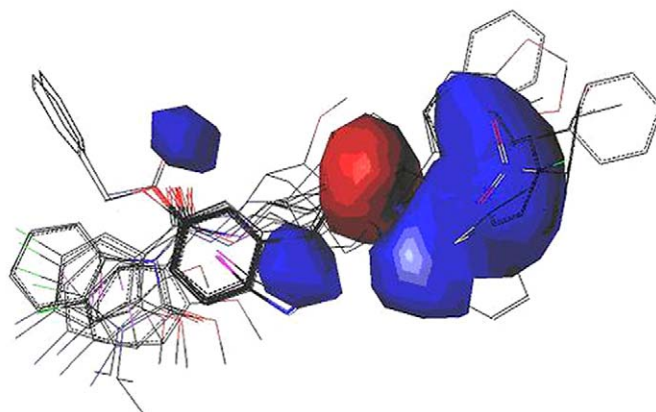


Fig. 5. Pharmacophore features developed from CoMFA Model B using the complete dataset; all the 23 compounds from Table 1: modified model using electrostatic anchor points: blue regions favor negative electrostatic charge; red regions favor positive electrostatic charge.

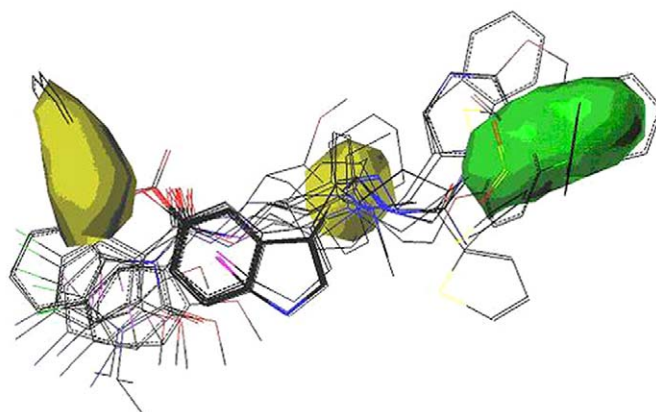


Fig. 6. Pharmacophore features developed from CoMFA Model B, modified model using electrostatic anchor points and the complete dataset from Table 1: yellow regions where steric bulk is unfavorable. Regions of favored steric bulk are colored green.

beyond the distant nitrogen anchor point is no longer a disordered clustering of various fields.

Pharmacophore model B (Fig. 7) shows the refined molecular alignment compared to model A alignment (Fig. 3). It positioned the aromatic ring system away from the traditional central location of the aromatic ring in model A. The CoMFA analysis indicated that this conformation was indeed favorable as there were no significant steric or electrostatic problems with accommodating the position of the tri-substituted aromatic ring of compounds **8**, **9**, **10**, **16**, **17**, **18** and **19**. The obtained data are shown in Table 2 column B.

4.3. Comparative analysis of models A and B

Comparative statistics and predicted values for 5-HT₄ agonists from the CoMFA analyses are shown in Table 2. Both A and B models are more complex than the initial one [9], with the number of components significantly increased due to a wider range of compounds used. Of interest, despite the modified positions of the aromatic rings of some of the ligands (**8**, **9**, **10**, **16**, **17**, **18** and **19**), their new locations are still sterically allowed, except for those pointing outwards from the hydroxyl group region (Fig. 6).

Model B indicated that the predictive power stems from far lower steric contributions, 0.270 compared to model A at 0.502. The dominant defining feature was the increase of electrostatic contributions for model B at 0.664 from 0.477 in model A. In both models the contributions from the LogP factor were minimal, 0.085 in model B.

The increase in contributions from the electrostatic term, both negative and positive, agrees well with the constructed 5-HT₄ binding site. In the binding site the residue serine 197 forms a strong hydrogen bond with the oxygen of the 5-hydroxyl group, the first alignment point, and the negatively charged aspartic acid 100 interacts with the positively charged tryptamine nitrogen. Agonists contain a secondary N rather than a positively charged nitrogen in the same location, a weaker but still significant interaction occurs as the secondary nitrogen still carries a lone pair of electrons and a slightly positive net charge.

The refined fields of the pharmacophore model B also allow us to see with greater confidence the groups and orientation of groups that are critical to high 5-HT₄ agonist activity, namely the hydrogen bond acceptor 5-hydroxyl group, the positive charge on the tryptamine nitrogen and for the first time the specific orientation of the lipophilic side chain beyond the

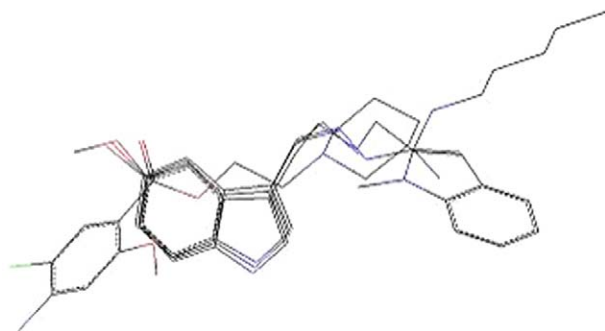


Fig. 7. CoMFA model B, a refined pharmacophore. Reduced dataset shown for simplicity, compounds shown are **1**, **4**, **7** and 5-HT.

charged nitrogen, angled upwards at about 60° out of the plane of the tryptamine ring system. The central aromatic ring was shown to be less significant, acting more as a spacer and scaffold to keep the two electrostatic groups at the correct distance and orientation from each other as well as steric bulk required by the binding site.

The agonists which did not contain a central tryptamine ring, such as the methoxybenzoate series, had their aromatic ring off the side below the 5-hydroxyl. In the constructed binding site the location of these aromatic rings was conveniently between two of the helices, forming further lipophilic interactions without being sterically constrictive. Utilizing the refined CoMFA model B which incorporate points from the binding site it is expected to provide a more defined pharmacophore for designing better 5-HT₄ agonists.

The two models (A and B) shared common features; the unfavorable steric region close to the 5-hydroxyl in yellow, the specific electrostatic favorable region close to the charged nitrogen in blue, the electrostatically unfavorable region beyond it in red and the steric favored region beyond it colored green Figs. 2,3 and 6. The steric, hydrophobic and aromatic rings stacking played a minor role in activity contributions.

CoMFA analysis molecular alignment of model A led to significantly different positioning of all of the compounds that contain the central tri-substituted aromatic ring such as zaco-

pride, cisapride and metoclopramide. Instead the negatively charged carboxyl oxygen and the nitrogen approximately 7–9 Å away were the key fitting points. This model placed the aromatic ring system away from the traditional fitting points, however the CoMFA analysis showed that there were no significant steric or electrostatic problems with accommodating the position of the tri-substituted aromatic ring. This finding was consistent with the analysis of the 5-HT₄ binding site and mutagenesis investigations [22,24]. A significant region below the 5-hydroxyl in the second model (B) is suitable for aromatic ring fitting as found in compounds like cisapride or zacopride where the steric bulk is unfavorable (colored yellow), regions of favored steric bulk are colored green (Fig. 6). Utilizing this new refined model one can better see the interactions involved of CoMFA contributions Table 3, where the electrostatic interactions were the dominant defining feature with the steric and lipophilic interactions being of less importance.

5. Conclusions

The modified CoMFA analysis (model B) agrees well with the constructed 5-HT₄ binding site. The CoMFA predictions of this modified model have confirmed the importance of electrostatic contributions for 5-HT₄ agonist activity. We have been able to use these recommendations for a new pharmacophore to design analogues with higher affinity and specificity. It must be noted that the series of compounds studied is limited and focused on developing a future robust model to discriminate between closely related receptors of the 5-HT₄ isoforms.

6. Pharmacological evaluation

Compounds were screened for 5-HT₄ agonist activity using a modification to the method described by Craig and Clarke [14]. Briefly, this involved measuring the ability of the compounds to increase the twitch responses of the guinea pig ileum myenteric plexus preparation, stimulated with single pulses of 1 ms duration at a frequency of 0.1 Hz with approximately

Table 3
CoMFA contributions of model B

	Steric Electrostatic Lipophilic LogP	Steric Electrostatic Lipophilic	Steric Electrostatic LogP	Steric Electrostatic	Steric LogP	Steric Lipophilic	Electrostatic Lipophilic	Electrostatic LogP
q^2	0.582	0.561	0.419	0.440	0.481	0.654	0.533	0.326
SEP	1.304	1.336	1.578	1.510	1.532	1.186	1.379	1.700
n	2	2	3	2	4	2	2	3
r^2	0.821	0.823	0.786	0.750	0.889	0.858	0.803	0.706
SEE	0.854	0.848	0.958	1.009	0.709	0.761	0.895	1.122
F	45.856	46.613	23.269	29.983	35.975	60.295	40.866	15.221
<i>Contributions</i>								
Steric	0.151	0.153	0.270	0.294	0.898	0.243	–	–
Electrostatic	0.380	0.385	0.644	0.706	–	–	0.452	0.906
Lipophilic	0.444	0.462	–	–	–	0.756	0.548	–
LogP	0.025	–	0.085	–	0.102	–	–	0.094

Statistical properties of PLS models using various CoMFA fields and LogP. The LOO cross-validated r^2 value is denoted q^2 . SEP is the standard error of prediction. n is the number of components used in the PLS analysis. r^2 is the non-cross-validated regression value. SEE is the standard error of estimation. F is the F -statistic for the analysis and contributions give the relative contributions for each of the fields used.

50% effective voltage. The tissues were bathed in Krebs Henseilt solution at 37 °C and bubbled continuously with a mixture of 95% O₂ and 5% CO₂. The modification involved adding ketanserin (10 µM) and tropisetron (10 µM) to the bathing solution to block 5-HT_{2A} and 5-HT₃ receptors, respectively. The preparations were loaded under a constant tension of 0.5 g and twitch responses were recorded isotonicly using force–displacement transducers (four-channel pen recorder, model 79D, Grass Instruments Co., Quincy, MA, USA).

The concentration–response curves of the compounds were constructed by exposing the strips to cumulative additions of the compounds at 0.5–1.0 min intervals. Each preparation was exposed to no more than six administrations to avoid desensitization.

6.1. Statistical analysis and reagents

Potencies of the agonists are expressed as relative to 5-HT (1.00) and intrinsic efficacy as E_{\max} values (full agonists, viz 5-HT = 1.00). These values were calculated by fitting the data points to a sigmoidal concentration–response curve of variable slope using non-linear regression using the program Graph Pad Prism (4.0). The following drugs were used: 5-HT creatine sulfate complex (Sigma-Aldrich Pty. Co., Castle Hill, Australia); ketanserin (Janssen-Cilag, Sydney, Australia) and tropisetron (Sandoz Ltd., Basle, Switzerland).

7. Chemistry

7.1. General

Reactions were monitored using thin layer chromatography (TLC) at 30 min intervals from the start to completion of reaction. The stationary phase was 0.2 mm aluminum backed Silica

Gel 60 F₂₅₄ sheets and the mobile phase was chloroform/methanol (95:5) unless otherwise stated. Nuclear magnetic resonance spectra were recorded on a Bruker AM-300 spectrometer at a frequency of 300 MHz. Chemical shifts (δ) are reported relative to tetramethylsilane at δ ppm. Mass spectra were recorded with a Micromass Platform spectrometer in electrospray mode at cone voltages 30, 70 and 100 eV. The following chemicals were purchased from Sigma-Aldrich Pty. Co.:

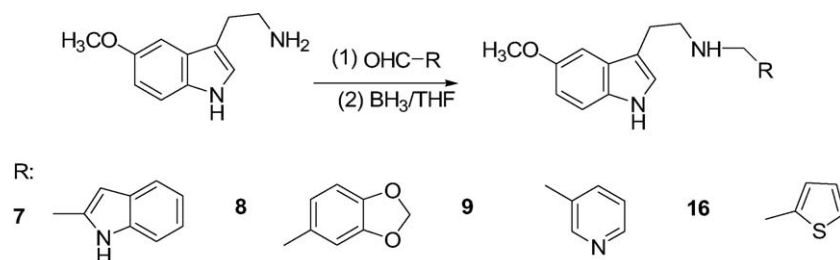
5-MeOT, 5-benzyloxytryptamine, thiophene-2-carboxaldehyde, pyrrole-2-carboxaldehyde, 2-thiophenecarbonyl chloride, 2-thiophenesulfonyl chloride, 2-thiopheneacetyl chloride, borane-tetrahydrofuran complex as 1.5 M solution in tetrahydrofuran and ether.

7.2. General methods

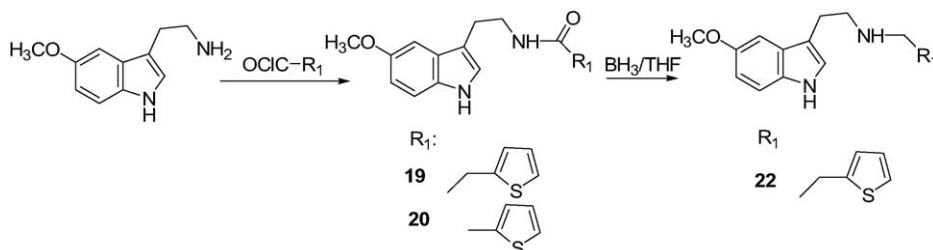
Three main methods (a, b and c) were used for the synthesis of the current compounds; aldehyde/amine, acid chloride/amine condensation and the products from these reaction were reduced with BH₃ (Schemes 1 and 2). These methods have generated compounds **7**, **8**, **9**, **16**, **17**, **18**, **19**, **20** and **22** in good yields.

7.2.1. Aldehyde and amine condensation

The appropriate aldehyde (1 mol equivalent) was added to dry methanol (10 ml) containing 5-MeOT (1 mol) and the mixture was refluxed under a nitrogen atmosphere for 3 h. The reaction mixture was then cooled to 0 °C, and the imine intermediate was reduced by the addition of NaBH₄ (3 mol) slowly and stirred for 30 min. The methanol was removed under reduced pressure and the organic crude was extracted with CDM, washed with 10% citric acid (10 ml), saturated solution of NaHCO₃ (10 ml), distilled water (20 ml), dried over anhydrous Na₂SO₄ and the organic solvent removed to yield the desired compound.



Scheme 1.



Scheme 2.

7.2.2. Acid chloride and amine condensation

The appropriate chloride compound (0.6 mmol) was added to dry CDM (10 ml) containing 5-MeOT (114 mg, 0.6) and triethylamine (83 mg, 0.8 mmol) at room temperature. The mixture was then refluxed under an atmosphere of nitrogen for 3 h. The solution was then cooled and washed with 10% citric acid saturated solution of sodium bicarbonate and distilled water. The CDM extract was dried over anhydrous Na_2SO_4 and the solvent removed under reduced pressure to give the desired product.

7.2.3. Amide reduction using BH_3

Borane (BH_3) in THF (2 ml, 1 M) was added slowly to dry THF (5 ml) containing the appropriate amide (0.30 mmol) at 0 °C under a nitrogen atmosphere. After the addition of BH_3 , the reaction mixture was refluxed for 4 h. THF was removed under reduced pressure and then NaOH (2 ml; 2.0 M) and CDM (20 ml) were added to the remaining residue. The organic layer was then washed with distilled water (20 ml \times 3) and dried over anhydrous Na_2SO_4 and concentrated down to give an oily brown product. The crude material was purified by using preparative TLC plates ($\text{CHCl}_3/\text{MeOH}$ 95:5).

Specific preparations are explained thereafter under individual compounds.

7.2.3.1. *N*-[2-(5-Methoxy-1*H*-indol-3-yl)ethyl],(*N*-methyl-1*H*-indol-2-yl)methanamine (7). This compound was prepared in 86% yield from 1-methylindole-2-carboxyaldehyde and 5-MeOT and reduction with BH_3 .

^1H NMR (300 MHz; DMSO): δ 2.81–2.89 (m, 4H, NCH_2CH_2), 3.270 (s, 3H, NCH_3), 3.70 (s, 3H, OCH_3), 5.68 (s, 2H, HNCH_2), 6.30 (s, 1H, H-3'), 6.68 (d, J = 8.7 Hz, 1H, H-6), 6.95–6.06 (m, 5H, H-2, -4, -3', -4' and H-6'), 7.19 (d, J = 8.7 Hz, 1H, H-7), 7.36 (d, J = 7.8 Hz, 1H, H-5'), 7.42 (d, J = 8.0 Hz, 1H, H-7'), 10.53 (s, 1H, ArNH).

ESMS m/z 334 [(M + 1)/1].

7.2.3.2. *N*-[2-(5-Methoxy-1*H*-indol-3-yl)ethyl],(1,3-benzodioxol-5-yl)methanamine (8). This compound was prepared from 1,3-benzodioxole-5-carboxyaldehyde and 5-MeOT and reduction with BH_3 , in 52% yield, ^1H NMR (300 MHz; DMSO): δ 2.86–2.91 (m, 2H, NCH_2), 3.45–3.52 (m, 2H, NCH_2CH_2), 3.71 (s, 3H, OCH_3), 6.07 (s, 2H, $(\text{CH}_2\text{O})_2\text{-CH}_2$), 6.70 (d, J = 6.6 Hz, 1H, H-6), 6.96 (d, J = 8.7 Hz, 1H, H-7), 7.03 (s, 1H, H-4'), 7.11 (s, 1H, H-2), 7.21 (d, J = 8.8 Hz, 1H, H-6'), 7.37 (s, 1H, H-4), 7.43 (d, J = 6.6 Hz, 1H, H-1'), 8.39 (s, 1H, ArNH).

ESMS m/z 313 [(M + 1)/1].

7.3. Preparation of *N*-[2-(methoxy-1*H*-indol-3-yl)ethyl]-*N*-(3-pyridinylmethyl)-1-ethanamine (9)

Prepared from nicotinoyl chloride hydrochloride and 5-methoxytryptamine and then the reduction of the product with BH_3 gave compound 9 as a light brown semi-solid product in 90% yield.

^1H NMR (300 MHz; CDCl_3): δ 3.22–3.49 (m, 4H, NCH_2CH_2), 3.74 (s, 3H, OCH_3), 6.68 (d, 1H, J = 8.40 Hz, H-6), 7.02 (s, 1H, H-2), 7.11 (s, 1H, H-4), 7.21 (d, 1H, J = 8.70 Hz, H-7), 7.47 (m, 1H, H-3'), 8.13 (d, J = 7.50 Hz, 1H, H-2'), 8.66 (s, 1H, H-4'), 8.91 (s, 1H, H-6'), and 8.93 (s, 1H, ArNH).

ESMS m/z 282 [(M + 1)/1].

7.3.1. *N*-[2-(5-Methoxy-1*H*-indol-3-yl)ethyl]-2-thiophenemethanamine (16)

Prepared in 82% yield from 2-thiophenecarboxaldehyde and 5-MeOT and the reduction with BH_3 .

^1H NMR (300 MHz; CDCl_3): δ 1.86 (s, 1H, NH), 2.95–3.06 (m, 6H, 2 \times NCH_2 and CH_2), 3.86 (s, 3H, OCH_3), 6.85 (s, 1H, H-2), 6.88–6.92 (m, 1H, H-6), 6.94 (d, J = 3.3 Hz, 1H, H-4), 7.00 (s, 1H, H-5'), 7.05 (s, 1H, H-4'), 7.20 (s, 1H, H-3'), 7.22 (d, J = 9.0 Hz, H-7), 7.97 (s, 1H, ArNH).

ESMS m/z 287 [(M + 1)/1].

7.3.2. *N*-[2-(5-Methoxy-1*H*-indol-3-yl)ethyl]-2-thiopheneacetamide (19)

Prepared in 60% yield from 2-thiopheneacetylchloride and 5-MeOT.

^1H NMR (300 MHz; CDCl_3): δ 2.89 (t, J = 6.6 Hz, 2H, CH_2), 3.52–3.59 (m, 4H, NCH_2 and COCH_2), 3.86 (s, 3H, OCH_3), 5.68 (s, 1H, NHCO), 6.80 (s, 1H, H-2), 6.84–6.86 (m, 1H, H-6), 6.89 (d, J = 2.4 Hz, 1H, H-4), 6.91–6.94 (m, 1H, H-4'), 7.20 (d, J = 5.1 Hz, 1H, H-3'), 7.26 (d, J = 9.3 Hz, H-7), 7.91 (s, 1H, ArNH).

ESMS m/z 315 [(M + 1)/1].

7.3.3. *N*-[2-(5-benzyloxy-1*H*-3-yl)ethyl]-2-thiophenecarboxamide (20)

Prepared in 65% yield from 2-thiophenecarbonylchloride benzyloxytryptamine.

^1H NMR (300 MHz; CDCl_3): δ 2.89 (t, J = 6.9 Hz, 2H, CH_2), 3.52–3.59 (m, 2H, NCH_2), 3.85 (s, 3H, OCH_3), 5.70 (s, 1H, NHCO), 6.80–6.88 (m, indolyl and phenyl-H), 6.91–6.93 (m, 1H, H-4'), 7.00 (s, 1H, H-5'), 7.20 (d, J = 5.1 Hz, 1H, H-3'), 7.22–7.26 (m, indolyl and phenyl-H), 7.97 (s, 1H, ArNH).

ESMS m/z 377 [(M + 1)/1].

7.3.4. *N*-[2-(5-Methoxy-1*H*-indol-3-yl)ethyl]-2-thiopheneethanamine (22)

Prepared in 56% yield by the BH_3 reduction of compound 19.

^1H NMR (300 MHz; CDCl_3): δ 3.02–3.06 (m, 4H, 2 \times CH_2), 3.71–3.78 (m, 7H, 2 \times NCH_2 and OCH_3), 6.28 (s, 3H, NH), 6.85 (d, J = 8.7 Hz, 1H, H-5'), 6.98–7.01 (m, 2H, H-6 and H-4), 7.05 (s, 1H, H-2), 7.24 (d, J = 8.7 Hz, 1H, H-7), 7.34–7.42 (m, 2H, H-3' and H-4'), 8.32 (s, 1H, ArNH).

ESMS m/z 301 [(M + 1)/1].

Acknowledgements

This work was funded by project grant from the National Health and Medical Research Council of Australia (NHMRC) and a scholarship to Mr. Ayad from the Faculty of Pharmacy, Monash University.

References

- [1] IUPHAR receptor data base, 2002. <http://iuphar-db.org/iuphar-rd/index.html>.
- [2] P.G. McLean, I.M. Coupar, P. Molenaar, Br. J. Pharmacol. 115 (1995) 47–56.
- [3] P.G. McLean, I.M. Coupar, Br. J. Pharmacol. 118 (1996) 1058–1064.
- [4] R.A. Borman, D.E. Burleigh, Eur. J. Pharmacol. 309 (1996) 271–274.
- [5] N.H. Prins, L.M.A. Akkermans, R.A. Lefebvre, J.A.J. Schuurkes, Br. J. Pharmacol. 131 (2000) 927–932.
- [6] S.A. Muller-Lissner, I. Fumagalli, K.D. Bardhan, Alimentary Pharmacol. & Ther. 15 (2001) 1655–1666.
- [7] M.J. Callahan, J. Clin. Gastroenterol. 35 (2002) S58–S67.
- [8] D. Hoyer, D.E. Clarke, J.R. Fozard, P.R. Hartig, G.R. Martin, E. J. Mylecharane, P.R. Saxena, P.P.A. Humphrey, Pharmacol. Rev. 46 (1994) 157–204.
- [9] M.N. Iskander, I.M. Coupar, D.A. Winkler, J. Chem. Soc. Perkin Trans. 2 (1999) 153–158.
- [10] K.H. Buchheit, R. Gamse, R. Giger, D. Hoyer, F. Klein, E. Kloppner, H. J. Pfannkuche, H. Mattes, J. Med. Chem. 38 (1995) 2331–2338.
- [11] D. Yang, J.L. Soulier, S. Sicsic, M. Mathe-Allainmat, B. Bremont, T. Croci, R. Cardamone, G. Aureggi, M. Langlois, J. Med. Chem. 40 (1997) 608–621.
- [12] T. Suzuki, N. Imanishi, H. Itahana, S. Watanuki, K. Miyata, M. Ohta, H. Nakahara, Y. Yamagiwa, T. Mase, Chem. Pharm. Bull. (Tokyo) 46 (1998) 1116–1124.
- [13] C.A. Rizzi, T. Coccini, L. Onori, L. Manzo, M. Tonini, J. Pharmacol. Exp. Ther. 261 (1992) 412–419.
- [14] D.A. Craig, D.E. Clarke, J. Pharmacol. Exp. Ther. 252 (1990) 1378–1386.
- [15] R.D. Cramer III, D.E. Patterson, J.D. Bunce, J. Am. Chem. Soc. 110 (1988) 5959–5967.
- [16] R.S. Bohacek, C. McMartin, J. Med. Chem. 35 (1992) 1671–1684.
- [17] SYBYL 6.9 Tripos Inc. 1699 South Hanley Road St. Louis, MO 63144-2319 www.tripos.com.
- [18] T. Halgren, J. Am. Chem. Soc. 112 (1990) 4710–4723.
- [19] T. Halgren, J. Comp. Chem. 20 (1999) 720.
- [20] S. Wold, C. Albano, W.J. Dunn III, U. Edlund, K. Esbensen, P. Geladi, S. Hellberg, E. Johansson, W. Lindberg, M. Sjostrom, “Multivariate data analysis in chemistry”, in: CHEMOMETRICS: Mathematics and Statistics in Chemistry, B. Kowalski, Reidel, Dordrecht, Netherlands, 1984.
- [21] G.R. Marshall, Binding-site modelling of unknown receptors. In 3D QSAR in Drug Design. Theory, Methods and Applications, in: H. Kubinyi (Ed.), Escom, Leiden, 1993, pp. 80–116.
- [22] M.L. Lopez-Rodriguez, B. Murcia, M. Benhamu, M. Olivella, M. Campillo, L. Pardo, J. Comput. Aided. Mol. Des. 15 (11) (2001) 1025–1033 (Nov).
- [23] G. Wishart, D.H. Bremner, K.R. Sturrock, Receptor Channels 6 (4) (1999) 317–323.
- [24] M.L. Lopez-Rodriguez, B. Murcia, M. Benhamu, M. Olivella, M. Campillo, L. Pardo, J. Comput. Aided. Mol. Des. 15 (11) (2001) 1025–1033 (Nov.).